

# Cell-Free Massive MIMO in the O-RAN Architecture: Cluster and Handover Strategies

Robbert Beerten, Vida Ranjbar, Andrea P. Guevara, Sofie Pollin

*Department of Electrical Engineering, KU Leuven, Belgium*

Corresponding Author: {robbert.beerten}@kuleuven.be

**Abstract**—Cell-free Massive MIMO has emerged as a promising solution for next-generation radio networks. Particularly the user-centric variant where users are served by a limited subset of access points, a so-called cluster, has garnered significant attention within the research community. Despite numerous proposed physical layer solutions, managing AP clusters in case of user mobility remains challenging. In this study, we first present a realistic method for modeling the temporal evolution of the channel in cell-free Massive MIMO. Next, we develop two clustering and handover strategies: 1) a fixed clustering strategy that computes the ideal cluster when a cluster handover threshold is exceeded and 2) an opportunistic strategy that opportunistically adds serving APs as the user moves. Moreover, we establish a connection between our findings and O-RAN, an emerging network architecture that offers open interfaces and network-wide control capabilities, thus, facilitating practical implementation of our research.

**Index Terms**—Cell-Free Massive MIMO, Distributed Processing, Next-Generation Radio Access Networks, Scalable Implementation, Dynamic Clustering

## I. INTRODUCTION

Cell-Free Massive MIMO (CF mMIMO) has emerged as a prominent enabler of next-generation networks, primarily due to its capacity to provide uniform service and exceptional coverage [1]. CF mMIMO refers to a network with many more Access Points (APs) than User Equipment (UEs), where APs cooperate via coherent joint transmission and reception. Recently, user-centric CF mMIMO [2] has gained considerable traction as the most promising variant of this technology. In this case, users are served by a limited subset of APs, a so-called cluster, that provide the best channel. However, efficiently managing these networks in the presence of user mobility remains a significant concern. While the problem was studied in [3]–[5], these works 1) lack a tractable channel model to study handover in sub-6GHz correlated Rayleigh fading and 2) rely on a single Central Processing Unit (CPU) for cluster reformulation and processing of the higher parts of the physical layer. Scalability of CF mMIMO networks was recently recognized as an important requirement [6]. The centralization of all computations in a single CPU should be avoided as this imposes immense requirements on the CPU’s fronthaul capacity and computing power. Hence, we provide

This research has received funding from the European Union’s Horizon 2020 research and innovation programme under Grant Agreement No. 101017171 (MARSAL project).

a method where APs can locally decide to serve UEs, thereby mitigating the computational burden on the CPU.

Splitting the CPU into multiple local computing units is also explored in [7]–[9]. Local signal estimates of these CPUs are then combined via different methods such as for example large-scale fading decoding.

This idea is reflected in our work, where multiple processing units (O-DUs) decode the signal collaboratively. Recently, O-RAN came forth as a promising approach to organise mobile networks. This new architecture proves to be interesting for practical deployments of CF mMIMO networks for two reasons. First, the physical layer is split between the O-RAN Distributed Units (O-DUs) and Radio Units (O-RUs) for the high PHY and low PHY, respectively. This is highly parallel to seminal papers on CF mMIMO where physical layer processing is split between the APs and the CPU. Multiple cooperating O-DUs can then be linked to theoretical CF mMIMO literature considering multiple cooperating CPUs. Second, extra functional blocks are introduced, enabling AI and containerized service orchestration on the network. These include the Near-Real Time RAN Intelligent Controller (Near-RT RIC), the Non-RT RIC, and the Service Management and Orchestration (SMO) framework. The functional split and options for network-wide control can achieve cooperation amongst O-RUs, even beyond the borders of the O-DUs. In this work, we show considerable synergy between these two and demonstrate that their combination can enable the next generation of wireless networks. This work will focus on how an O-RAN network can achieve cooperation and smooth handover between its O-DUs via our proposed inter-O-DU interface, the E2 interface and the Near-RT RIC.

**Contribution:** This paper makes three key contributions to the current state-of-the-art. First, we propose a tractable temporal channel model for CF mMIMO at sub6-GHz frequencies. Second, we study the problem of handover in CF mMIMO and introduce two strategies: an opportunistic clustering strategy, where APs can locally decide to serve specific users, and a fixed clustering strategy, where handover is computed at a central processor. Our work establishes a framework that includes our notions of primary O-RU, primary O-DU and serving and measurement cluster. Third, we extend our previous work [10] and map our handover solutions to a real network architecture and offer practical implementation guidelines. Thus, this work bridges theory and practice by

linking the algorithms to the O-RAN architecture.

*Notation:* A diagonal matrix with the elements  $x_i$  on the main diagonal is denoted by  $\text{diag}(x_0, x_1, \dots, x_N)$ . The cardinality of a set  $\mathcal{S}$  is written as  $|\mathcal{S}|$ . For matrices and vectors alike,  $\mathbf{A}^T$  is the transpose,  $\mathbf{A}^H$  is the Hermitian conjugate of the matrix, and  $\mathbf{A}^*$  is the complex conjugate. The  $l$ 'th element of vector  $\mathbf{a}$  is denoted by  $[\mathbf{a}]_l$ . The expected value of  $x$  is denoted by  $\mathbb{E}\{x\}$ .

## II. CLUSTER FORMATION

In this work, we consider a scenario with  $K$  UEs,  $C$  O-DUs,  $L$  O-RUs with  $N$  antennas each and a single Near-RT RIC. We also denote the set of O-RUs that are connected to O-DU  $c$  as  $\mathcal{L}_c$ . When a UE first connects to the network, it selects a **primary O-RU**, and the O-DU that controls that O-RU logically becomes the primary O-DU. This choice is based on the channel gain that the UE computes based on a DL pilot<sup>1</sup>. The concept of the primary O-RU is important as it determines **handover** and the **measurement cluster**. We define handover as a transition to a new primary O-RU. The measurement cluster,  $\mathcal{M}_k^m$ , consists of the O-RUs closest to that UE's primary O-RU on which the channel gain for a specific UE  $k$  is measured. Subsequently, the **serving cluster**  $\mathcal{M}_k^s$  are formed as a subset of  $\mathcal{M}_k^m$  by using one of the two cluster formation algorithms explained in the following subsections. This serving cluster performs joint precoding/decoding for a specific UE  $k$ . Note that these O-RUs in  $\mathcal{M}_k^s$  can belong to one or multiple O-DUs, thus, potentially requiring O-DUs to cooperate. We also define  $\mathcal{D}_l$  as the set of all UEs that are served by O-RU  $l$ . Two strategies for determining **serving clusters** are proposed: a *fixed* serving cluster formation and an *opportunistic* serving cluster formation. We compare these two methods against two baselines, ubiquitous CF and a cellular system with a single O-DU serving.

### A. Fixed Cluster Formation

After the primary O-RU, O-DU and measurement cluster are determined, the O-DUs that control O-RUs in the measurement cluster report the UL channel gains,  $\beta_{l,k}$ , between those O-RUs  $l$  and UE  $k$  to the Near-RT RIC. To determine the serving cluster, we define  $O_k[t]$  as the function that selects the subset of  $|\mathcal{M}_k^s|$  O-RUs in the measurement cluster that experience the highest UL channel gains from UE  $k$  at time  $t$ . These serving O-RUs then become the serving cluster. Next, the sum of DL channel gains from the initial serving cluster to UE  $k$ , is determined as  $\bar{P}_k$  at the UE. This metric represents the total signal quality in the cluster when it is created and plays a crucial role in the handover mechanism, which will be discussed in Section IV. The main advantage of this method is that the number of O-RUs,  $|\mathcal{M}_k^s|$ , can be controlled by the Near-RT RIC. The main disadvantage is the substantial signaling between the O-DUs and the Near-RT RIC.

<sup>1</sup>We see this as a valid assumption as many works have argued in favour of DL pilots for DL signal processing, which is out of scope for this paper yet important for CF mMIMO systems [11].

### B. Opportunistic Cluster Formation

By the opportunistic method, after the allocation of the primary O-RU and O-DU, O-DUs can decide autonomously if they serve a specific UE on O-RUs with available resources without involving the Near-RT RIC. In this case, the Near-RT RIC serves as a bookkeeper and to inform the O-DUs about two things. First, O-DUs must be aware of which O-DUs serve as primary O-DU for UEs they serve themselves. Second, they must know which UEs have its O-RUs in their measurement cluster. Both of these only change in the case of primary O-RU changes. These message are necessary such that an O-DU knows with which O-DU it should instantiate an inter-O-DU interface for cooperative decoding and to limit the number of UEs an O-DU keeps track of. Thus, this method has very limited requirements in terms of signaling. O-DUs decide opportunistically by only selecting O-RU - UE pairs with the highest UL channel gains. The O-DUs prioritise pairs of UEs with primary O-RUs rather than opportunistic serving. [2] also proposes a clustering scheme where O-RUs can decide locally if they serve a specific UE but do not explore how to change these UE - O-RU associations in case of UE mobility. To limit the size of the serving cluster, we restrict the size of the measurement cluster and also limit the number of UEs a specific O-RU can serve to  $N$ . In contrast to the fixed clustering strategy, this opportunistic strategy avoids a network-wide procedure executed at the Near-RT RIC. The function  $Q_l^{(w)}[t]$  maps all UEs whose measurement cluster contains O-RU  $l$  to the subset of  $w \leq N$  UEs that achieve the best channel towards O-RU  $l$  at time  $t$ . This function loads an O-RU up to its limit, including the UEs that use it as primary O-RU i.e. an O-RU that currently serves  $K_l^*$  UEs as primary O-RU could take an additional  $N - K_l^*$  UEs opportunistically. Algorithm 1 shows how O-RUs can be maximally loaded. The main advantage of this method is the low computational cost and signaling load. The main disadvantage of this method is that there are no guarantees on the number of serving O-RUs beyond the primary O-RU.

---

#### Algorithm 1 Initial Opportunistic Cluster Formation

---

```

1: for  $k = 1 \dots K$  do
2:   Assign primary O-RUs
3:    $l_k^* = \arg \max_l \beta_{l,k}[0]$ 
4: end for
5: for  $l = 1 \dots L$  do
6:   Load each O-RU upto  $N$  UEs
7:    $\mathcal{D}_l[0] \leftarrow Q_l^{(N-K_l^*)}[0]$ 
8: end for

```

---

### C. Baselines

By the ubiquitous method, every UE is served by every single O-RU in the network and thus  $|\mathcal{M}_k^s| = L$ . We use this as an upper bound on the performance of the clustering. By comparing to the optimal, ubiquitous case, we can evaluate the performance gap to a heuristic handover scheme. For the

cellular case, every UE is served only by O-RUs connected to a single O-DU. This is used as a lower bound on the performance to show the benefits of implementing our proposed inter-O-DU interface. The disadvantages are two-fold; first the amount of O-RUs is inherently limited due to the size of the O-DU; second, the set is rarely optimal due to the high probability of O-RUs from a different O-DU providing a better channel than the selected O-RUs.

### III. SYSTEM MODEL

This section describes UL detection, channel estimation, and combiner calculation during a specific coherence block. We use a method from the current state-of-the-art and map it to the O-RAN architecture. Subsections III-A, III-B, and III-C use the method proposed in [12, Ch. 4-5]. In Section III-D, we extend our system to allow for mobility of the UEs and how to temporally evolve our channel model.

#### A. Channel Model

In this work, we consider UL detection. The channel vector between a single-antenna UE  $k$  and an O-RU  $l$ ,  $\mathbf{h}_{l,k} \in \mathbb{C}^N$ , is generated from a complex normal distribution,

$$\mathbf{h}_{l,k} \sim \mathcal{CN}(\mathbf{0}, \mathbf{R}_{l,k}). \quad (1)$$

Where  $\mathbf{R}_{l,k} \in \mathbb{C}^{N \times N}$  is the covariance matrix of the channel. We assume these  $\mathbf{R}_{l,k}$  to be known at the respective O-DU for that O-RU  $l$ . We will later link these  $\mathbf{R}_{l,k}$  to our mobility model in Section III-D.

#### B. Channel Estimation

To estimate the channel, the UEs transmit mutually orthogonal pilot sequences  $\phi_i \in \mathbb{C}^{\tau_p}$ . In the UL, UE  $k$  transmits pilot  $\phi_{t_k}$  in the designated time slot, where  $t_k$  is the index of the pilot allocated to UE  $k$ . O-RU  $l$  receives the superposition of all of the UEs' pilots as  $\mathbf{Y}_l \in \mathbb{C}^{N \times \tau_p}$ :

$$\mathbf{Y}_l = \sum_{k=1}^K \sqrt{p_k} \mathbf{h}_{l,k} \phi_{t_k}^T + \mathbf{N}_l. \quad (2)$$

Where  $\mathbf{N}_l$  is a matrix with the measured noise realizations  $\mathbf{n}_{t,l}$  in the columns. Each of its elements are i.i.d. distributed white noise from the distribution  $\mathcal{CN}(0, \sigma_{\text{ul}}^2)$ . The O-DU decorrelates these received pilots for UE  $k$  in O-RU  $l$  as  $\mathbf{y}_{l,k}^{(p)} = \mathbf{Y}_l \frac{\phi_{t_k}^*}{\sqrt{\tau_p}}$ . The O-DU then calculates the MMSE channel estimates between UE  $k$  and O-RU  $l$ ,  $\hat{\mathbf{h}}_{l,k}$ , as

$$\hat{\mathbf{h}}_{l,k} = \sqrt{\tau_p p_k} \mathbf{R}_{l,k} \left( \sum_{i \in \mathcal{P}_k} \tau_p p_i \mathbf{R}_{l,i} + \sigma_{\text{ul}}^2 \mathbf{I}_N \right)^{-1} \mathbf{y}_{l,k}^{(p)}. \quad (3)$$

We denote the error on the channel estimate as  $\tilde{\mathbf{h}}_{l,k} = \hat{\mathbf{h}}_{l,k} - \mathbf{h}_{l,k}$ . The covariance of the channel estimation error is  $\mathbf{C}_{l,k}$ .

#### C. Receive Combining

Large-Scale Fading Decoding (LSFD) fits nicely into the O-RAN architecture. UL detection has three stages in our system. First, each O-RU  $l$  estimates the signal  $\hat{s}_{l,k}$  of its served UEs locally and sends these local estimates to its respective O-DU. Second, this O-DU  $c$  computes more accurate estimates for the UE's signal  $\hat{s}_k^c$  based on its LSFD weights which the primary O-DU then combines into the final estimate for the UE's signal,  $\hat{s}_k$ . This mapping of LSFD to O-RAN was proposed in [10] and relies on the interface between cooperating O-DUs which was proposed in [13]. The received signal at each O-RU is,

$$\mathbf{y}_l = \sum_{k=1}^K \mathbf{h}_{l,k} s_k + \mathbf{n}_l. \quad (4)$$

In our analysis, we use the Local Partial MMSE (LP-MMSE) combiner as it is computed separately for each O-RU by the relevant O-DU. The O-DU computes an LP-MMSE receive combiner  $\mathbf{v}_{l,k}$  for each of its O-RU - UE associations,

$$\mathbf{v}_{l,k} = p_k \left( \sum_{i \in \mathcal{D}_l} p_i \left( \hat{\mathbf{h}}_{l,i} \hat{\mathbf{h}}_{l,i}^H + \mathbf{C}_{l,i} \right) + \sigma_{\text{ul}}^2 \mathbf{I}_N \right)^{-1} \hat{\mathbf{h}}_{l,k}. \quad (5)$$

The O-DU computes this combiner only if  $k \in \mathcal{D}_l$ . Otherwise we take  $\mathbf{v}_{l,k} = \mathbf{0}_{N \times 1}$ . The O-RU then locally combines the received signal via  $\mathbf{v}_{l,k}$  as,

$$\hat{s}_{l,k} = \mathbf{v}_{l,k}^H \mathbf{y}_{l,k}, \quad \forall l \in \mathcal{M}_k^s. \quad (6)$$

We compute cluster-wide LSFD combining weights for the local O-RU estimates.  $\mathbf{g}_{ki}$  is the effective gain for UE  $i$  in the receive combiner for UE  $k$  and  $\delta_{l,k}$  indicates if UE  $k$  is served by O-RU  $l$  i.e.  $\mathbf{g}_{ki} = [\mathbf{v}_{1,k}^H \mathbf{h}_{1,i} \ \mathbf{v}_{2,k}^H \mathbf{h}_{2,i} \ \dots \ \mathbf{v}_{L,k}^H \mathbf{h}_{L,i}]^T$ . We denote the set of UEs that share at least one O-RU with UE  $k$  as  $\mathcal{S}_k$ . We use so-called n-opt LSFD [12], where it is assumed that only those UEs in  $\mathcal{S}_k$  induce significant interference for UE  $k$ , and thus only those UEs are considered in the LSFD combiner. The primary O-DU can calculate the LSFD weights  $\mathbf{a}_k \in \mathbb{C}^L$  as [12],

$$\mathbf{a}_k = p_k \left( \sum_{i \in \mathcal{S}_k} \mathbb{E}\{\mathbf{g}_{ki} \mathbf{g}_{ki}^H\} + \mathbf{F}_k \right)^{-1} \mathbb{E}\{\mathbf{g}_{kk}\}. \quad (7)$$

Where  $\mathbf{F}_k = \sigma_{\text{ul}}^2 \text{diag}(\mathbb{E}\{\|\mathbf{v}_{1,k}\|\}, \dots, \mathbb{E}\{\|\mathbf{v}_{L,k}\|\})$ . The weight vector for UE  $k$ ,  $\mathbf{a}_k$ , has  $|\mathcal{M}_k^s|$  non-zero elements, one for each O-RU that is serving UE  $k$ . The LSFD weights are only a function of the statistics of the channels and channels are independent, so it is sufficient to compute the local mean gains for each O-RU to determine the overall weights [12, p.323]. This decreases the inter-O-DU signalling for computing the LSFD combiner significantly. Because, instead of continuously sending effective gains, only the expected values of these effective gains must be transmitted. We consider the statistics on these effective gains to be known at the O-DU for each UE that is served by its' O-RUs, these are then

transmitted to the relevant primary O-DUs over our inter-O-DU interface. O-DU  $c$  combines the signals locally for each UE served by O-RU  $l \in \mathcal{L}_c$  as

$$\hat{s}_k^c = \sum_{l \in \mathcal{L}_c} [\mathbf{a}_k^*]_l \hat{s}_{l,k}. \quad (8)$$

The primary O-DU then computes the final estimate for the UE's signal by combining the estimates of each of the serving O-DUs,  $\hat{s}_k^c$  as  $\hat{s}_k = \sum_c \hat{s}_k^c = \sum_{l \in \mathcal{M}_k^s} [\mathbf{a}_k^*]_l \hat{s}_{l,k}$ . The result is then transparent to how the O-RUs are organised amongst the different O-DUs. The SINR is estimated as [14, Eq. 5.26],

$$\gamma_k^{\text{ul}} = \frac{p_k |\mathbf{a}_k^H \mathbb{E}\{\mathbf{g}_{kk}\}|^2}{\mathbf{a}_k^H (\sum_{i \in \mathcal{S}_k} p_i \mathbb{E}\{\mathbf{g}_{ki} \mathbf{g}_{ki}^H\} - p_k \mathbb{E}\{\mathbf{g}_{kk}\} \mathbb{E}\{\mathbf{g}_{kk}^H\} + \mathbf{F}_k) \mathbf{a}_k} \quad (9)$$

The SE is then estimated as:  $\text{SE}_k^{\text{ul}} = \log_2(1 + \gamma_k^{\text{ul}})$ , which is used in Section VI for performance evaluation.

#### D. Proposed Temporal Channel Model

Next, we explain how the channel model can be evolved temporally. The UEs move in a straight line at constant speed  $v_k$  at a random angle. The sample time of the simulation is  $T_S$ . If the deployment of O-RUs is dense, a minor movement of a UE induces a significant change in the Angle of Arrival (AoA) for the received signal at an O-RU and thus changes the covariance matrix of the channel significantly (see Eq. 13). In [3], individual NLOS paths are updated via Jakes autocorrelation model. The autocorrelation coefficient is computed with a zero'th order Bessel J function as follows

$$\rho = J_0(\pi D_s T_s). \quad (10)$$

Where  $D_s = 2f_c \frac{v}{c}$  is the doppler spread of the received signal. This function tends to zero even for relatively small  $T_s$  in the context of cluster formation. Hence, this model generates almost purely random channels. We propose a model more suitable for larger sampling times where even the NLoS paths are not strongly correlated. We expect the large-scale fading to be correlated. Hence, we model shadow fading as an autoregressive function. In [15], the spatial auto-correlation function for shadow fading is formulated as  $e^{-\alpha d}$ , where  $\alpha$  is the reciprocal of the decorrelation distance and  $d$  the distance between the two considered points. We take  $\alpha$  to be  $(20\text{m})^{-1}$  which is the recommended value for a typical European city [15]. A UE moves a distance of  $v_k T_S$  between two subsequent samples. We model the shadow fading  $F_{l,k}[t]$  at time  $t$  as,

$$F_{l,k}[t] = \rho_k F_{l,k}[t-1] + \sqrt{1 - \rho_k^2} F_{l,k}^{\text{new}}. \quad (11)$$

Where  $\rho_k = e^{-\alpha v_k T_S}$  is the correlation coefficient for two subsequent realizations,  $F_{l,k}^{\text{new}}$  is a newly drawn shadow fading from the distribution  $\mathcal{N}(0, \sigma_{\text{sf}}^2)$ . The large scale fading is then modelled as,

$$\beta_{l,k}^{\text{dB}}[t] = -34 - 38 \log_{10}(d_{l,k}[t]) + F_{l,k}[t]. \quad (12)$$

Where  $d_{l,k}$  is the distance between a specific UE  $k$  and O-RU  $l$  expressed in meters. The channel covariance matrices are regenerated at every new time instance. To calculate the

second-order statistics of the channel, we use the one-ring scattering model [16] to calculate the element at row  $m$  and column  $n$  of the covariance matrix,

$$[\mathbf{R}_{l,k}]_{m,n}[t] = \beta_{l,k}[t] \int e^{2\pi j d_H(n-m) \sin(\bar{\phi}_{l,k})} f(\bar{\phi}_{l,k}, t) d\bar{\phi}_{l,k}, \quad (13)$$

where  $f(\bar{\phi}_{l,k}, t)$  is the time-dependent distribution of the possible angles of arrival between user  $k$  and O-RU  $l$ . For this work, we consider a uniform distribution and thus,  $\bar{\phi}_{l,k} = \phi_{l,k} + \delta$ ,  $\delta \sim U[-\xi, \xi]$ , where  $\phi_{l,k}$  is the true angle of arrival, and  $\xi$  models the richness of the scattering environment.

## IV. HANDOVER

We consider a network where a UE is served by only a subset of the O-RUs in the network and is moving. Thus, any selected subset of O-RUs will become suboptimal as the UE moves away from its cluster. Hence, in this section, we propose updating strategies for the clusters from Section II. We discuss these handover procedures at discrete times  $t$ , which are spaced apart at the same intervals,  $T_s$ . When the UE triggers a *primary O-RU handover*, it selects a new primary O-RU, and thus O-DU, with the highest DL channel gain. The corresponding primary O-DU then requests a new measurement cluster around the new primary O-RU. Every time we sample the clusters, we first check if a new cluster is needed, possibly update the cluster and then always update the LSFD weights.

#### A. Handover for Fixed Clustering

By the fixed clustering strategy, the UE monitors the instantaneous total received power of the cluster  $P_k[t]$ , via a DL control channel and triggers a handover if it is significantly below the initial cluster power, i.e.  $P_k[t] < \bar{P}_k - M_{\text{HO}}^F$ , where  $M_{\text{HO}}^F$  is a hysteresis threshold. The UE then chooses a new primary O-RU and O-DU. The measurement cluster is then also updated by the Near-RT RIC. Subsequently, the Near-RT RIC determines a new serving cluster for that UE. The threshold brings a trade-off in the system's performance (higher SE) versus less signaling overhead (less frequent handovers).

#### B. Opportunistic Cluster Tracking

We also define a handover strategy for our opportunistic clustering. In opportunistic tracking, the cluster updates on two different levels: 1) The primary O-RU which is triggered by the UE; 2) The opportunistic serving decisions by the O-DUs. Every UE is connected to one O-RU as its primary one, denoted by  $l_k^*$ . A change of the primary O-RU requires the UE to perform an actual handover. To limit the signaling between the O-DUs and the Near-RT RIC, it is logical to make the UE responsible for the handover of its primary O-RU as it is the UE's only persistent connection. A UE triggers a primary O-RU handover when it detects a significantly higher DL channel gain to a different O-RU in its measurement cluster (line 4 in Alg. 2). If the new primary O-RU exceeds its limit of served UEs due to that handover, that O-RU drops the weakest UE

it is currently serving opportunistically (line 5-8 in Alg. 2). When the primary O-RU is updated, the measurement cluster changes accordingly, i.e. the closest O-RUs to the new primary O-RU become the new measurement cluster. Additionally, an O-DU dynamically changes the set of UEs it opportunistically serves on its O-RUs with resources not occupied by primary O-RU connections. The O-DUs constantly track the path loss between its O-RUs and UEs in its measurement clusters and choose to serve the best ones (line 13-17 Alg. 2). Any changes in the opportunistic serving set do not change any connections between UEs and their primary O-RU.

We introduce the handover threshold as  $M_{HO}^O$  and design it to be the same for the handover of the primary O-RU which is triggered by the UE and the opportunistic serving of extra UEs. However, we do acknowledge that it might be interesting to use different thresholds for the primary handover and opportunistic O-RU reload and consider it an important direction for future work. We show the procedure Algorithm 2.

#### Algorithm 2 Opportunistic Cluster Tracking

```

1: At every time t
2: for  $k = 1 \dots K$  do
3:    $\bar{l} \leftarrow \arg \max_l \beta_{l,k}^{\text{dB}}$ 
4:   if  $(\beta_{\bar{l},k}^{\text{dB}}[t] > \beta_{l_k^*,k}^{\text{dB}}[t] + M_{HO}^O) \wedge (\bar{l} \neq l_k^*)$  then
5:     Primary O-RU handover
6:      $\mathcal{D}_{l^*}[t] \leftarrow Q_{l^*}^{(N-K_l^*+1)}[t]$ 
7:      $l_k^* \leftarrow \bar{l}$ 
8:      $\mathcal{D}_{\bar{l}}[t] \leftarrow Q_{\bar{l}}^{(N-K_{\bar{l}}^*)}[t]$ 
9:   end if
10:  end for
11:  for  $l = 1 \dots L$  do
12:    if  $\exists k \notin \mathcal{D}_l[t] : \beta_{l,k}^{\text{dB}}[t] > \beta_{l,k}^{\text{dB}}[t] + M_{HO}^O, k \in \mathcal{D}_l[t]$  then
13:      Opportunistic O-RU Reload
14:       $\mathcal{D}_l[t] \leftarrow Q_l^{(N-K_l^*)}[t] \cup \{k : l_k^* = l\}$ 
15:    else
16:       $\mathcal{D}_l[t] \leftarrow \mathcal{D}_l[t - 1]$ 
17:    end if
18:  end for

```

#### C. Baselines

By the ubiquitous method, the UE is served by all O-RUs. The UE can move anywhere without significant losses because the LSFD combiner can calculate new combining weights  $\mathbf{a}_k$  based on the changing channel. Hence, there is no handover needed. However, it is helpful to highlight the performance gap to this method. By the cellular method, a UE requests a handover when it detects that it has a significantly higher DL channel gain to an O-RU in a different O-DU than the one by which it is currently served based on a hysteresis threshold.

#### V. CONTROL AND DATA PLANE

In this section, we give a brief comparison of the signalling costs associated with the different methods. For UL data plane processing, the values are derived from [12]. O-RU  $l$  needs to

signal  $\tau_u$ , which is the number of data symbols in a coherence block, samples to the O-DU for every user  $k$  in  $\mathcal{D}_l$ . These are then combined in the O-DU to  $\tau_u$  samples of  $\hat{s}_k^c$  for every unique user served by the O-DU. For every UE  $k$  O-DU  $c$  is serving as a primary O-DU, O-DU  $c$  receives  $\tau_u$  samples for every unique O-DU that controls the O-RUs in the set  $\mathcal{M}_k^s \setminus (\mathcal{M}_k^s \cap \mathcal{L}_c)$ . Additionally, for every UE  $k$  they are serving but not as primary O-DU, O-DUs transmit  $\tau_u$  samples  $\hat{s}_k^c$

For cluster formation, the costs vary significantly for the two methods. For the fixed method, every time the UE triggers a handover, the O-DUs in the measurement cluster must transmit  $|\mathcal{M}_k^m|$  UL path loss  $\beta_{l,k}$  measurements to the Near-RT RIC. So in the worst case, if every user triggers a handover at the same time, the traffic to the Near-RT RIC reaches  $|\mathcal{M}_k^m|K$ . The opportunistic method only requires the new primary O-RUs to notify the Near-RT RIC of its UEs.

#### VI. SIMULATION AND NUMERICAL RESULTS

We quantify the performance of the different clustering and handover methods. We provide the ubiquitous case as an upper bound and the cellular case as a lower bound on the performance; for this case, we use a hysteresis parameter of 2 dB. The parameters for the simulation are listed in Table I. The O-RUs are located in a square grid, this grid is divided into uniformly sized squares for each O-DU, the O-RUs for a specific O-DU are then placed randomly in the subsquare for its O-DU via a uniform distribution. The UEs are then also randomly placed in the grid according to a uniform distribution. To ensure consistent performance across the simulation area, we replicated the initial setup eight times, resulting in a wrap-around scenario with a  $3 \times 3$  tile configuration.

| Parameter              | Value    | Parameter       | Value |
|------------------------|----------|-----------------|-------|
| $K$                    | 40       | $L$             | 36    |
| $N$                    | 4        | $C$             | 9     |
| $\sigma_{\text{ul}}^2$ | -94 dBm  | $\tau_p$        | 100   |
| Grid Size              | 1 x 1 km | $T_s$           | 0.5s  |
| Number of Setups       | 25       | $\xi$           | 10°   |
| $ \mathcal{M}_k^s $    | 16       | Simulation Time | 10s   |

TABLE I: Simulation Parameters

#### A. Handover Frequency

Figure 1 quantifies the handover frequency for different speeds and different threshold values ( $M_{HO}^O$  and  $M_{HO}^F$ ). Fixed clustering, which is expensive for the Near-RT RIC, exhibits a lower handover frequency than opportunistic clustering for the same threshold. This is attributed to the tracking of cluster-wide channel gain which is less sensitive to the UE’s mobility than the channel gain for only the primary O-RU. For both methods, the number of handovers increases with speed and decreases with a rising threshold. This highlights a vital trade-off, a high frequency of handovers improves the SE significantly, especially for high speeds. This becomes expensive for fixed clustering as the Near-RT RIC becomes very loaded with handover procedures whereas the opportunistic cluster tracking only requires minor signaling.

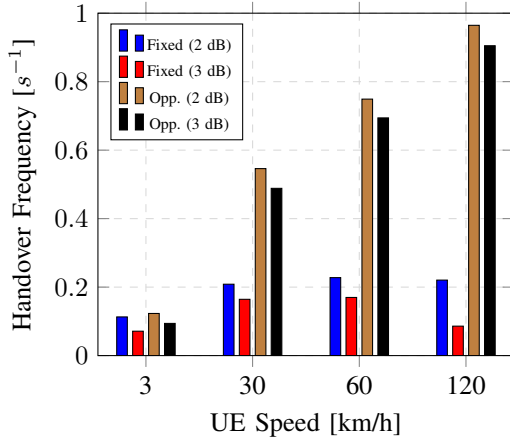


Fig. 1: Handover frequency for the different methods for two different thresholds ( $M_{HO}^O/M_{HO}^F$ ) and varying UE's speeds.

### B. Mean Spectral Efficiencies

Figure 2 illustrates the influence of the threshold on the mean spectral efficiency (SE) as a function of UE speed. For the fixed clustering, the mean SE drops with increasing UE speed and even more so if the HO threshold is chosen too large. In our setup, performance then degrades beyond that of the opportunistic method. The performance of the opportunistic clustering is less sensitive to the threshold value than the fixed clustering due to the UE only triggering handover if the total received power decreases too much in the fixed clustering. The opportunistic clustering allows a new O-RU to easily start serving a new UE when that O-RU detects it as sufficiently strong. Hence, the opportunistic strategy provides more fine-grained control. This does, however, come at the cost of not having a deterministic number of O-RUs that serve a particular UE as it is impossible for our algorithm to guarantee any quality of service beyond that provided by the primary O-RU. Furthermore, the ubiquitous case is barely affected by increasing speed of the UE.

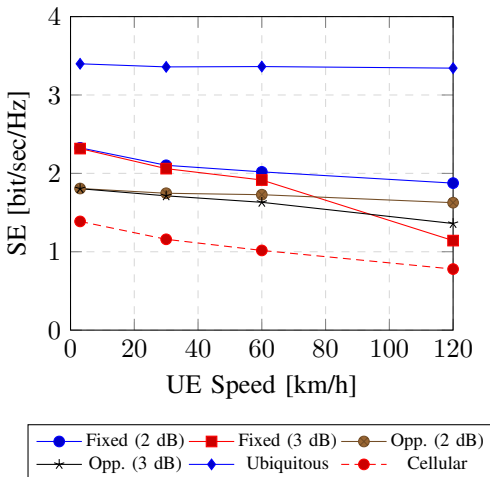


Fig. 2: Mean SE for different UE speeds

## VII. CONCLUSION

In this work, we have introduced a novel temporal channel for correlated Rayleigh fading in CF mMIMO networks. We introduced two clustering and handover strategies, mapped them to the O-RAN architecture and benchmarked them via our selected UL detection method based on the mean SE. We find that the opportunistic clustering provides more fine-grained control than the fixed clustering strategy in the presence of UE mobility. Furthermore, we have demonstrated that CF mMIMO is much more resilient against UE mobility compared to classical cellular systems.

## REFERENCES

- [1] E. Nayebi, A. Ashikhmin, T. L. Marzetta, and H. Yang, "Cell-Free Massive MIMO systems," in *2015 49th Asilomar Conference on Signals, Systems and Computers*, 2015, pp. 695–699.
- [2] S. Buzzi and C. D'Andrea, "Cell-Free Massive MIMO: User-Centric Approach," *IEEE Wireless Communications Letters*, vol. 6, no. 6, p. 706–709, Dec. 2017.
- [3] C. D'Andrea, G. Interdonato, and S. Buzzi, "User-centric Handover in mmWave Cell-Free Massive MIMO with User Mobility," in *2021 29th European Signal Processing Conference (EUSIPCO)*, Aug. 2021, p. 1–5.
- [4] M. Zaher, E. Björnson, and M. Petrova, "Soft Handover Procedures in mmWave Cell-Free Massive MIMO Networks," no. arXiv:2209.02548, Sep. 2022, arXiv:2209.02548 [eess]. [Online]. Available: <http://arxiv.org/abs/2209.02548>
- [5] Y. Xiao, P. Mähönen, and L. Simić, "Mobility Performance Analysis of Scalable Cell-Free Massive MIMO," no. arXiv:2202.01488, Feb. 2022, arXiv:2202.01488 [cs, math]. [Online]. Available: <http://arxiv.org/abs/2202.01488>
- [6] E. Björnson and L. Sanguinetti, "Scalable Cell-Free Massive MIMO Systems," *IEEE Transactions on Communications*, vol. 68, no. 7, p. 4247–4261, Jul. 2020.
- [7] G. Interdonato, P. Frenger, and E. G. Larsson, "Scalability Aspects of Cell-Free Massive MIMO," in *ICC 2019 - 2019 IEEE International Conference on Communications (ICC)*, May 2019, p. 1–6.
- [8] F. Li, Q. Sun, X. Ji, and X. Chen, "Scalable Cell-Free Massive MIMO with Multiple CPUs," *Mathematics*, vol. 10, no. 11, p. 1900, Jun. 2022.
- [9] F. Riera-Palou and G. Femenias, "Decentralization Issues in Cell-free Massive MIMO Networks with Zero-Forcing Precoding," in *2019 57th Annual Allerton Conference on Communication, Control, and Computing (Allerton)*, Sep. 2019, p. 521–527.
- [10] R. Beerten, A. Girycki, and S. Pollin, "User Centric Cell-Free Massive MIMO in the O-RAN Architecture: Signalling and Algorithm Integration," in *2022 IEEE Conference on Standards for Communications and Networking (CSCN)*, pp. 181–187.
- [11] G. Interdonato, H. Q. Ngo, P. Frenger, and E. G. Larsson, "Downlink Training in Cell-Free Massive MIMO: A Blessing in Disguise," *IEEE Transactions on Wireless Communications*, vol. 18, no. 11, p. 5153–5169, Nov. 2019, arXiv: 1903.10046.
- [12] Ö. T. Demir, E. Björnson, and L. Sanguinetti, "Foundations of User-Centric Cell-Free Massive MIMO," *Foundations and Trends® in Signal Processing*, vol. 14, no. 3-4, pp. 162–472, 2021. [Online]. Available: <http://dx.doi.org/10.1561/2000000109>
- [13] V. Ranjbar, A. Girycki, M. A. Rahman, S. Pollin, M. Moonen, and E. Vinogradov, "Cell-Free mMIMO Support in the O-RAN Architecture: A PHY Layer Perspective for 5G and Beyond Networks," *IEEE Communications Standards Magazine*, vol. 6, no. 1, p. 28–34, Mar. 2022.
- [14] Ö. T. Demir, E. Björnson, and L. Sanguinetti, "Cell-Free Massive MIMO with large-scale fading decoding and dynamic cooperation clustering," in *WSA 2021; 25th International ITG Workshop on Smart Antennas*. VDE, 2021, pp. 1–6.
- [15] Z. Wang, E. Tameh, and A. Nix, "Joint Shadowing Process in Urban Peer-to-Peer Radio Channels," *IEEE Transactions on Vehicular Technology*, vol. 57, no. 1, p. 52–64, Jan. 2008.
- [16] E. Björnson, J. Hoydis, and L. Sanguinetti, "Massive MIMO Networks: Spectral, Energy, and Hardware Efficiency," *Foundations and Trends® in Signal Processing*, vol. 11, no. 3-4, pp. 154–655, 2017. [Online]. Available: <http://dx.doi.org/10.1561/2000000093>